

Sliding Mode Observer of a Power Quality in Grid Connected Renewable Energy Systems

A. Djeriou^{*‡}, K.Aliouane^{**}, F.Bouchafaa^{*}

^{*} Laboratory of Instrumentation, Faculty of Electronics and Computer, University of Sciences and Technology Houari Boumediene, BP 32 El-Alia 16111 Bab-Ezzouar Algiers, Algeria

^{**} UER Electrotechnique, EMP, BP 17 Bordj-El-Bahri, Algiers, Algeria

alidjeriou@yahoo.fr, kam-ali@lycos.com, fbouchafa@gmail.com

[‡] Corresponding Author; A. Djeriou, BP 32 El-Alia 16111 Bab-Ezzouar Algiers, Algeria, 021.247.187,alidjeriou@yahoo.fr

Received: 16.06.2012 Accepted: 05.08.2012

Abstract- The first problem in our third millennium is energy. For this reason, we try to find a new solution to develop different ways of distribution and energy use. This article presents the design of a sliding mode controller using sliding mode observation technique which aims to simplify the control procedure. For ameliorating the quality of the energy transferred from the power supply to the load, and minimizing the harmful effects of the harmonics generated by nonlinear load. The virtual grid flux vector estimated in the sliding-mode observer yields robustness against the line voltage distortions. We propose a new multi-function converter as an efficient solution to improve the power quality. The good dynamic and static performance under the proposed control strategy is verified by simulation and experiment.

Keywords- Harmonics, Three phase APF, PWM rectifier, DPC, virtual line flux linkage observer, MVBPF, PV, sliding mode(SM), SMO (Sliding Mode Observer).

1. Introduction

Photovoltaic is the most direct way to convert solar radiation into electricity. The generation of electricity is based on the photovoltaic effect, which was first observed by Henri Becquerel [6] in 1839. It is the technological symbol for a future sustainable energy supply system in many countries. A considerable amount of money is invested in research, development and demonstration; several governments set up substantial market introduction programs and industry invests in larger production facilities. This is a remarkable situation since at the same time photovoltaic (PV) electricity is regarded as much too expensive compared to conventional grid electricity.

Sliding mode observation and control schemes for both linear and nonlinear systems have caused considerable interest in recent times. Discontinuous nonlinear control and observation schemes, based on sliding modes, exhibit fundamental robustness and insensitivity its properties of great practical value [1].

For ultimate goal of reducing the overcrowding and elevate the performance in treating the energy of power system. This work gives a supplementary function to power converter for making sure it work also an active filter.

2. Custom Power Devices

All custom power devices are capable of providing a number of power quality functions which can be employed selectively or simultaneously.

2.1. Control of PWM Rectifier with Active Filtering Function

Nowadays, harmonic pollution in electrical power systems due to nonlinear loads such as AC-to-DC power converters has become a serious problem.

To eliminate or reduce harmonics in the power systems, a number of methods have been developed and put into practice. Active power filters and PWM rectifiers are two typical examples of these methods. The active power filter

and PWM rectifier have basically the same circuit configuration and can operate based on the same control principle.

Sliding-mode current observer for virtual grid flux

The aim of Virtual Flux (VF) approach is to improve the VOC (Voltage Oriented Control) [2]. The Sliding-Mode Direct Power Control technique with the pseudo-sliding mode DC-link voltage controller presented in Fig (1) has

been examined in the simulation and experimental research. For the PWM rectifier the inductor voltages v_L and the converter input voltages v_f balance the grid voltages v_s according to the matrix equation

$$v_s = v_L + v_f \tag{1}$$

The (a-b) components of the converter voltage vector v_f can be estimated out of the dependence involving the DC-link voltage and the PWM pattern:

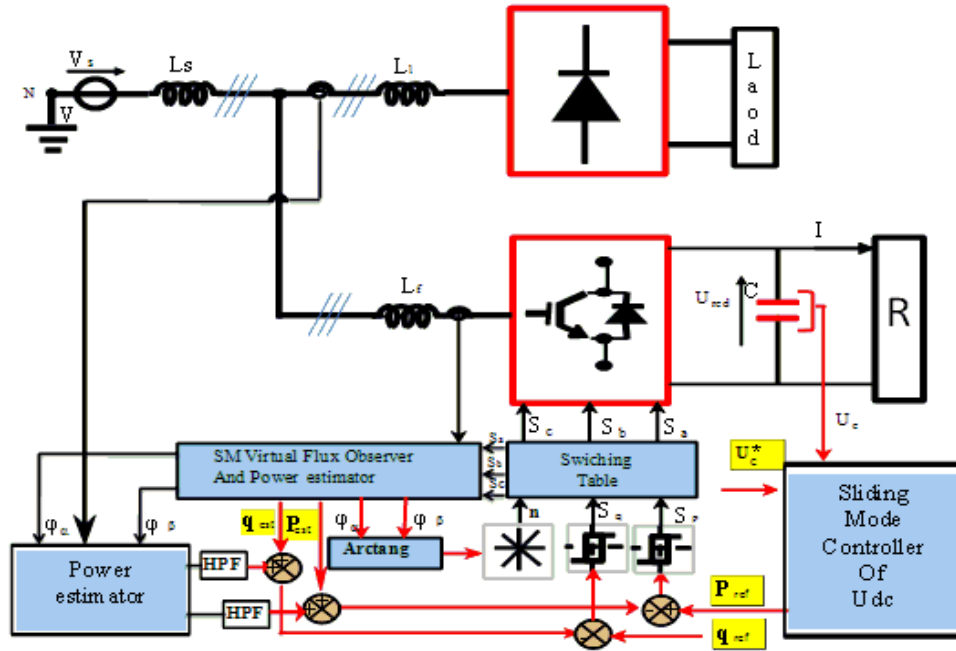


Fig.1. Control of PWM Rectifier with Active Filtering Function based on sliding-mode observers

$$\begin{cases} v_{f\alpha} = \sqrt{\frac{2}{3}} U_c \left(S_a - \frac{1}{2}(S_b + S_c) \right) \\ v_{f\beta} = \sqrt{\frac{2}{3}} U_c (S_b - S_c) \end{cases} \tag{2}$$

The sliding mode observer uses the system model with model with the sign feedback function. The continuous time version of the SMO (Sliding Mode Observer) is described by Equation (3).

$$\frac{d}{dt} \begin{bmatrix} i_{f\alpha} \\ i_{f\beta} \end{bmatrix} = \frac{1}{L_f} (\lambda \cdot \text{sign} \begin{bmatrix} i_{f\alpha} - i_{faest} \\ i_{f\beta} - i_{fbest} \end{bmatrix}) - R_f \begin{bmatrix} i_{f\alpha} \\ i_{f\beta} \end{bmatrix} - \begin{bmatrix} v_{f\alpha} \\ v_{f\beta} \end{bmatrix} \tag{3}$$

The estimated values of the grid voltage are obtained from the low-pass filter:

$$\begin{bmatrix} v_{saestSMO} \\ v_{s\beta estSMO} \end{bmatrix} = LPF(\lambda \cdot \text{sign} \begin{bmatrix} i_{f\alpha} - i_{faest} \\ i_{f\beta} - i_{fbest} \end{bmatrix}) \tag{4}$$

While the (α - β) components of the virtual grid flux are calculated as follows:

$$\begin{bmatrix} \varphi_{\alpha est} \\ \varphi_{\beta est} \end{bmatrix} = (\lambda \int \text{sign} \begin{bmatrix} i_{f\alpha} - i_{faest} \\ i_{f\beta} - i_{fbest} \end{bmatrix} dt) + \begin{bmatrix} \varphi_{\alpha est0} \\ \varphi_{\beta est0} \end{bmatrix} \tag{5}$$

Where λ is the positive constant

Hence the structure of the virtual grid flux sliding-mode observer presented in Fig.2.

$$\begin{bmatrix} \sigma_\alpha \\ \sigma_\beta \end{bmatrix} = \begin{bmatrix} i_{f\alpha} - i_{faest} \\ i_{f\beta} - i_{fbest} \end{bmatrix} \tag{6}$$

The sliding mode will exist only if the following condition

$$\begin{cases} \dot{\sigma}_\alpha \sigma_\alpha < 0 \\ \dot{\sigma}_\beta \sigma_\beta < 0 \end{cases} \tag{7}$$

The instantaneous active and reactive powers are estimated in the block (power observer) by measurement of line current and the estimation of the virtual flux components φ_{fa} , φ_{fb} [13].

$$\begin{cases} P_{Cest} = \omega (\varphi_{aest} \cdot i_{fb} - \varphi_{\beta est} \cdot i_{fa}) \\ Q_{Cest} = \omega (\varphi_{aest} \cdot i_{fa} - \varphi_{\beta est} \cdot i_{fb}) \end{cases} \tag{8}$$

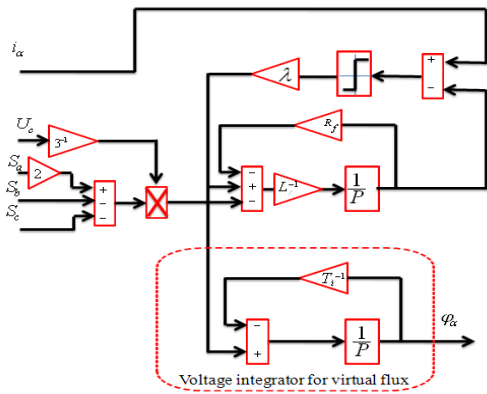


Fig.2. Sliding-mode current observer for virtual grid flux

Table 1. Switching Table

S _p	S _q	θ ₁	θ ₂	θ ₃	θ ₄	θ ₅	θ ₆	θ ₇	θ ₈	θ ₉	θ ₁₀	θ ₁₁	θ ₁₂
1	0	V ₆	V ₇	V ₁	V ₀	V ₂	V ₇	V ₃	V ₀	V ₄	V ₇	V ₅	V ₀
	1	V ₇		V ₀			V ₇		V ₀		V ₇		V ₀
0	0	V ₆	V ₁	V ₂		V ₃		V ₄		V ₅		V ₆	
	1	V ₁	V ₂	V ₃		V ₄		V ₅		V ₆		V ₁	

With: V₀(000), V₇(111), V₁(100), V₂(110), V₃(010), V₄(011)
 V₅(001), V₆(101).

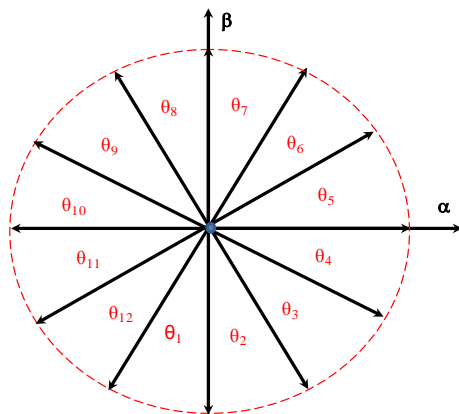


Fig.3. Virtual flux plane 12 sectors

The figure 3 shows the 12 voltage sectors plane for switching table.

2.2. Sliding Mode Control of a Grid Connected Photovoltaic Generation System with Active Filtering Function

The motivation for this work was to design a digitally controlled, combination active filter and photovoltaic (PV) generation system. This work focuses on a proposed control scheme for the dual function system and on the effects of delay on the control of an active filter. The scheme of the proposed multi-function converter is shown in Fig.5

A. Modelling of the PVG

The mathematical model of the PVG is given by model 1.

The command reactive power q_{ref} and (delivered from the outer sliding mode DC-link voltage controller) active power P_{ref} values are compared with the estimated q and p values, in reactive and active powers hysteresis controllers, respectively.

$$\begin{aligned} &\text{If } (q_{ref} - q > H_q), d_q = 1; \text{ Else, } d_q = 0; \\ &\text{If } (p_{ref} - p > H_p), d_p = 1; \text{ Else } d_p = 0; \end{aligned} \quad (7)$$

H_p and H_q are the hysteresis band. Table I shows the switching table for VF-DPC control.

$$I = I_{sc} - I_0 \left[e^{\left(\frac{V + IR_{sr}}{nkT_c/q} \right)} - 1 \right] - \frac{V + IR_{sr}}{R_{sh}} \quad (8)$$

With I and V are respectively the PV current and voltage, I₀:leakage or reverse saturation current, q: electron charge, n: Ideality factor, K is the Boltzman's constant (1.38.10⁻²³ J/K), R_{sr}:series cell resistance, R_{sh}:shunt cell resistance.

B. Boost converter

The Boost converter shown in Figure 4, it has step-up conversion ratio. Therefore the output voltage is always higher than the input voltage. The converter will operate throughout the entire line cycle, so the input current does not have distortions and continuous. It has a smooth input current because an inductor is connected in series with the power source. In addition the switch is source-grounded; therefore it is easy to drive.

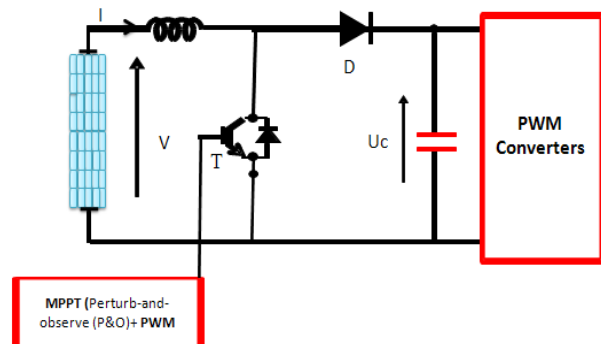


Fig.4. Boost converter

B. Mathematical Model of PWM Converters

A three phase voltage inverter is used to interface the PVG with the grid by converting the dc power generated by the PVG into AC power to be injected to the grid. The

dynamic model of a PWM DC-AC Converter can be described in the well known (d-q) frame through the Park transformation as follows [1], see appendix:

$$\begin{aligned} \frac{di_{fd}}{dt} &= \frac{-R_f}{L_f} i_{fd} + \omega i_{fq} + \frac{1}{L_f} v_{fd} - \frac{v_{sd}}{L_f} \\ \frac{di_{fq}}{dt} &= \frac{-R_f}{L_f} i_{fq} + \omega i_{fd} + \frac{1}{L_f} v_{fq} - \frac{v_{sq}}{L_f} \\ \frac{dU_c}{dt} &= \frac{d_d}{C} i_{fq} + \frac{d_q}{C} i_{fd} \end{aligned} \quad (9)$$

Where

d_d, d_q d- Axis and q- axis switching state functions,
 \hat{v}_{sd} and \hat{v}_{sq} - d- Axis and q- axis supply voltages.

The bi-directional characteristic of the converter is very important in this proposed photovoltaic system, because it allows the processing of active and reactive power from the generator to the load and vice versa, depending on the application. Thus, with an appropriate control of the power switches it is possible to control the active and reactive power flow.

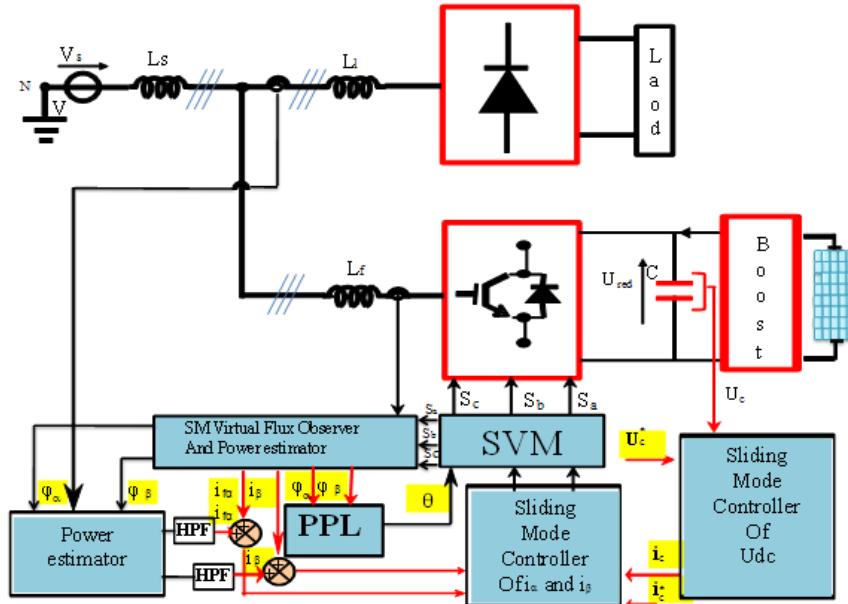


Fig.4. Scheme of the multi-function converter

$$\begin{bmatrix} \hat{v}_d \\ \hat{v}_q \end{bmatrix} = \frac{1}{i_{fd}^2 + i_{fq}^2} \begin{bmatrix} i_{fd} & -i_{fq} \\ i_{fq} & i_{fd} \end{bmatrix} \begin{bmatrix} P \\ Q \end{bmatrix} \quad (10)$$

Where \hat{v}_d and \hat{v}_q are the estimated main line

C. The regulators Synthesis

The state equations are shown in (11) and summarized as (12)

$$\begin{bmatrix} \frac{di_{fd}}{dt} \\ \frac{di_{fq}}{dt} \end{bmatrix} = \begin{bmatrix} \frac{-R_f}{L_f} & \omega \\ -\omega & \frac{-R_f}{L_f} \end{bmatrix} \begin{bmatrix} i_{fd} \\ i_{fq} \end{bmatrix} + \begin{bmatrix} \frac{1}{L_f} \\ \frac{1}{L_f} \end{bmatrix} \begin{bmatrix} v_{fd} \\ v_{fq} \end{bmatrix} - \begin{bmatrix} \frac{v_{sd}}{L_f} \\ \frac{v_{sq}}{L_f} \end{bmatrix} \quad (11)$$

$$\dot{i} = AI + Bu - G \quad (12)$$

The sliding surfaces (S) are equal to the error of state variables, which can be express as:

$$S = K_{SMP} E_f + K_{SMI} \int E_f dt \quad (13)$$

Where

$$\begin{aligned} S &= \begin{bmatrix} S_d \\ S_q \end{bmatrix}; E_f = I^* - I; I^* = \begin{bmatrix} i_{fd}^* \\ i_{fq}^* \end{bmatrix}; \\ K_{SMP} &= \begin{bmatrix} k_{SMPd} & 0 \\ 0 & k_{SMPq} \end{bmatrix}; K_{SMI} = \begin{bmatrix} k_{SMId} & 0 \\ 0 & k_{SMIq} \end{bmatrix} \end{aligned}$$

Where k_{SMPd} , k_{SMPq} , k_{SMId} and k_{SMIq} and 3 are positive constants and consequently, their temporal derivatives are given by:

$$\dot{S} = K_{SMP} \dot{E}_f + K_{SMI} E_f \quad (14)$$

The equivalent control can be calculated from the formula $\dot{S} = 0$, and the stabilizing control is given to guarantee the convergence condition (13).

$$\dot{S} = K_{SMP} \dot{I}^* + K_{SMI} E_f - K_{SMP} (AI + Bu - G) = 0 \quad (15)$$

The equivalent control u_{eq} is deduced by imposing the sliding regime condition $\dot{S} = 0$ obtaining:

$$u_{eq} = \begin{bmatrix} u_{eqd} \\ u_{eqq} \end{bmatrix} = (K_{SMP} B)^{-1} \left[K_{SMI} E_f - K_{SMP} (AI + Bu - G + \dot{I}^*) \right] \quad (16)$$

Finally, the control law is given by:

$$u = u_{eq} + u_{dis} = \begin{bmatrix} u_{eqd} + u_{disd} \\ u_{eqq} + u_{disq} \end{bmatrix} = \begin{bmatrix} u_{eqd} + k_{sd} \text{sign}(S) \\ u_{eqq} + k_{sq} \text{sign}(S) \end{bmatrix} \quad (17)$$

For the sliding mode DC-link voltage controller based on integrator can be determined by substituting the reference line current, is chosen to determine switching surface functions:

$$S_{dc} = K_{SMPC}(U_c^* - U_c) + K_{SMIC} \int (U_c^* - U_c) dt \quad (18)$$

And consequently, their temporal derivative is given by:

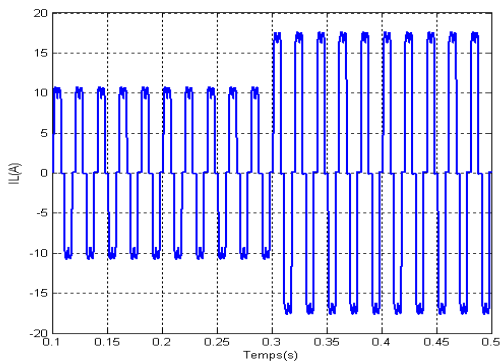
$$\dot{S}_{dc} = K_{SMPC}(\dot{U}_c^* - \dot{U}_c) + K_{SMIC}(U_c^* - U_c) = 0 \quad (19)$$

Finally, the control law is given by:

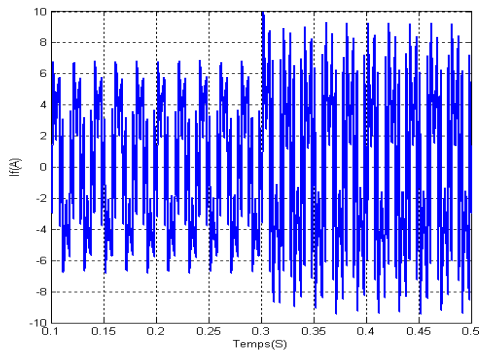
$$i_{ceq} = C \left(\frac{K_{SMIC}}{K_{SMPC}} (U_c^* - U_c) + \dot{U}_c^* \right) + K_{SC} \text{sign}(U_c^* - U_c) \quad (20)$$

3. Simulation Result

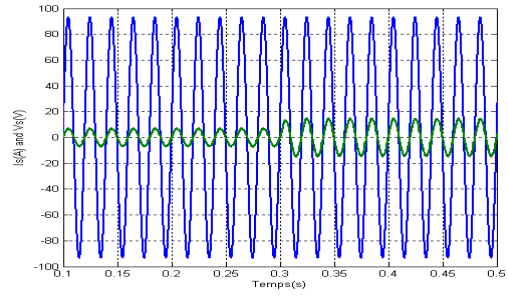
In simulation part, power system is modeled as 3wired 3-phase system by an RL load with uncontrolled diode rectifier. In the circuit, the ac source with frequency of 50Hz. The grid side line voltage is 220V. The line resistor is 0.25Ω. The line inductance of each phase is 1mH. The dc capacitor is 5000μF; the dc voltage is set to be 700V. The switching frequency for three-phase is 15 kHz.



(a)



(b)



(c)

Fig.5. Simulated responses for a step change in the load resistor: a) Load current before filtering Load change at 0.3s. b) Harmonic currents injected by the PWM Rectifier, c) Source voltage, source current.

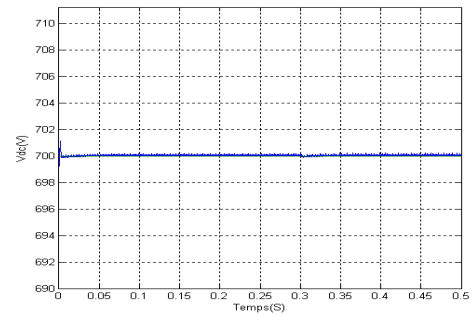


Fig. 6. DC side capacitor voltage and filter current

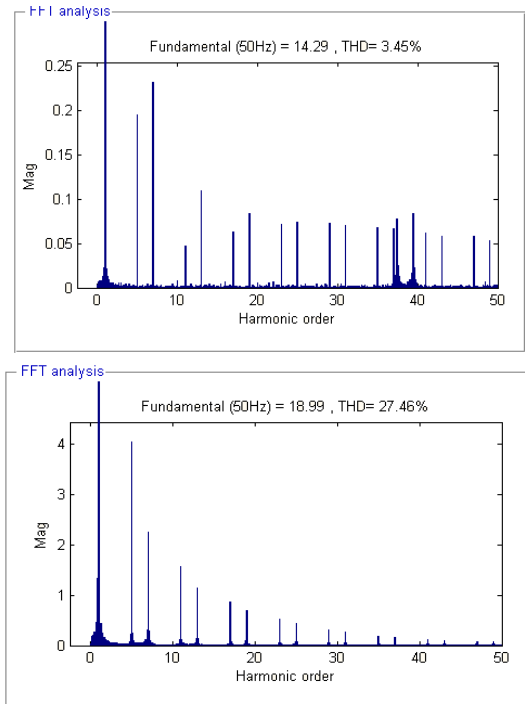


Fig.7. Current spectrum harmonic: Grid and Load in Phase 1.

The Pv model applied in simulation is as Fig.4. Whose parameters are regulated for normal condition (25⁰ C Temp. and sun radiation G=1kW/m).

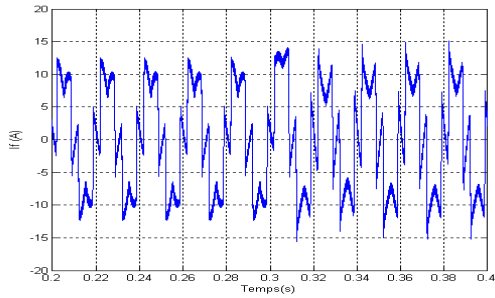
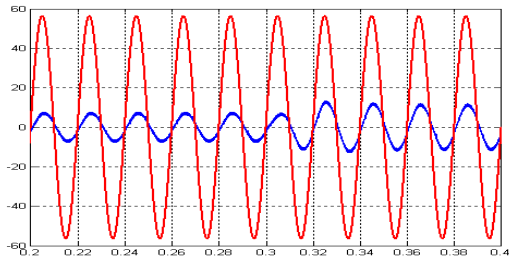
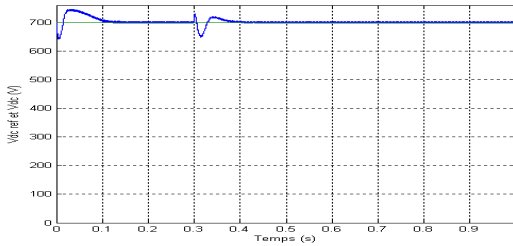


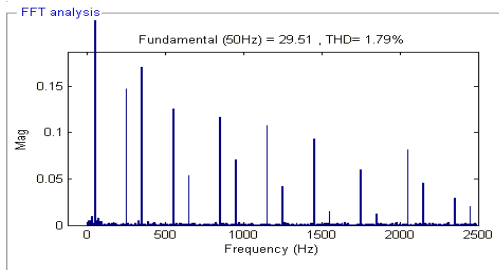
Fig.8. Harmonic currents injected by the active power filter.



(a)



(b)



(c)

Fig.9. Simulated responses for a step change in the load resistor: a) Source voltage, source current. b) DC side capacitor voltage and filter c) Current spectrum harmonic: Grid in Phase 1.

Control of PWM Rectifier with Active Filtering Function

Fig. 5.A. shows the simulated one phase current load waveform with a step at time 0.3 s.

The current reference of the PWM rectifier and the generated one are superposed in the same Fig. (7).

Fig.5.C. Fig.6.Presents the start up the PWM rectifier operation. It is noted the linear currents are sinusoidal and the control technique presents a very good dynamic behavior, This thanks to SM regulator behavior used control the DC-link voltage. Under APF operation, the line current

becomes almost sinusoidal as well as in phase with line voltage, which gives near-to-unity power factor.

Fig.7. shows the source current spectrum analysis before and after filtering. Before filtering; one can see the current harmonics distortion value was $THDi = 27.46\%$ and after filtering it will be $THDi = 3.45\%$. Secondly; to show the performance during transient condition the load current is changed at 0.3 s.

Sliding Mode Control of a Grid Connected Photovoltaic Generation System with Active Filtering Function

The current reference of the active filter and the generated one are superposed in the same Fig. (8).

The Fig. 9.A. shows the behavior of the current and voltage in Phase 1 of the grid,. It is noted the linear currents are sinusoidal and the control technique presents a very good dynamic behavior, almost sinusoidal as well as in phase with line voltage, which gives near-to-unity power factor.

Fig. 9.B. shows simulation results for the DC bus voltage controller. The voltage vdc on the DC side of the inverter is stable and regulated around its reference.

The THD before filtering for the first line is 27.46 % and becomes 1.79% after filtering.

4. Experimental Results

Due to the computational constraints of the TMX320lf2407 fixed-point DSP used in the experimental setup of the PWM rectifier. The sliding-mode-current observers for the grid voltage and the virtual grid flux have been validated experimentally in the linear control systems presented in Fig.10.



Fig.10. PWM Rectifier With the function of an Active Power Filter experimental test bench

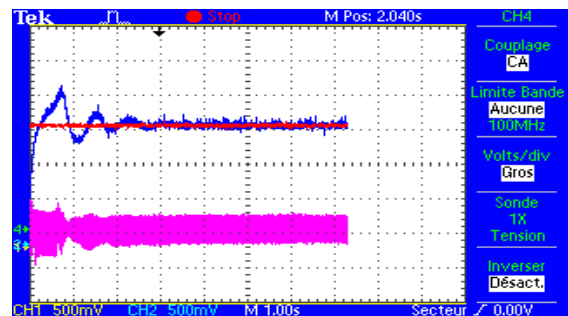


Fig.11. DC-link voltage variation current sag. detected

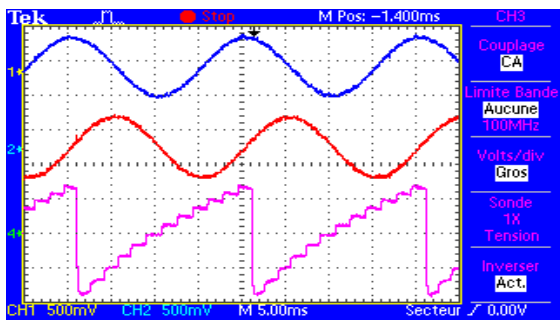


Fig.12. Sector detected.(d) Positive-sequence VF

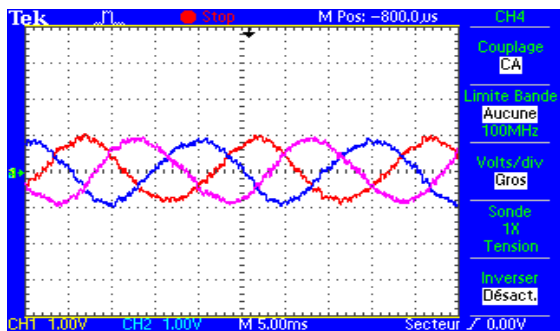


Fig.13. Operation of PWM Rectifier under grid and active

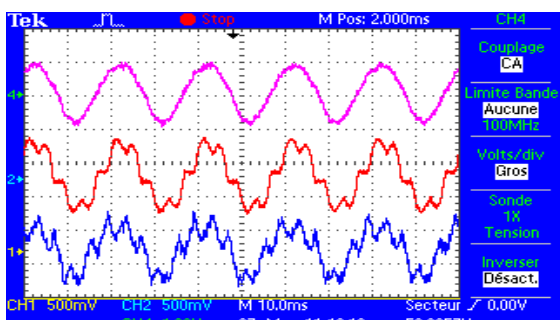


Fig.14. From top to bottom current ac source current filter current

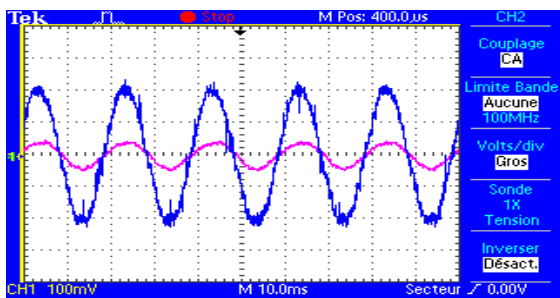


Fig.15. PWM rectifier operation without filtering operation [line voltage (v) and line current (i)].

5. Conclusion

This paper outlined the modeling and development of the control system for the active filter/PV generation system and PWM rectifier with sliding mode controller based on a Sliding Mode Observer. The results verify the validity of the proposed control scheme. Unity power factor is achieved, active and reactive current are decoupled controlled in the synchronous reference frame and the objective of

maintaining balanced voltages in DC-link capacitors is carried out effectively with the proposed SVM, and it offers sinusoidal line currents (low THD) for ideal and distorted line voltage.

The SMO_DPC system constitutes a viable alternative to the conventional control strategies and it has the following features and advantages.

- No line voltage sensors are required;
- It has a lower sampling frequency (than a conventional
- DPC [13]).
- It has good dynamics.
- It offers sinusoidal line currents (low THD), for ideal and distorted line voltage.
- No current control internal loops
- Decoupled active and reactive power control
- Robustness to grid voltage distortions.

References

- [1] C.Canudes de Wit and J.J.E. Soltine, "Sliding Observers for Robot Manipulators," Automatica, 1991 vol 27 pp 859-864
- [2] A. Kheloui, K. Aliouane, "A Fully Digital Vector Current Control of Three Phase Shunt Active Power Filters", IECON2002 0-7803-7474-6/02/\$17.00 ©2002 IEEE
- [3] A. Chaoui, J.P. Gaubert, F. Krim, L. Rambault, Power quality improvement using DPC controlled three-phase shunt active filter, ScienceDirect (10.1016/j.epr.2009.10.020)
- [4] K. Hasan, and K. Osman, "Globally Stable Control of Three-Phase Three Wire Shunt Active Power Filters," Elec. Eng., vol. 89, no.5, 2007, pp. 411-418.
- [5] Helder J. Azevedo, José M. Ferreira, António P. Martins, and Adriano S. Carvalho "Direct current control of an active power filter for harmonic elimination, power factor correction and load unbalancing compensation," Proceedings of the 10th European Conference on Power Electronics and Applications, EPE'03, Toulouse, 2003, pp. 1-10.
- [6] Becquerel AE, Comt Rend. Academie d. Sciences 9 (1839) p. 561
- [7] Antonio P. Martins, "The use of an active power filter for harmonic elimination and power quality improvement in a nonlinear loaded electrical installation", Proceedings of the International Conference on Renewable Energies and Power Quality, ICREPQ'03, Vigo, 2003, pp. 1-6.
- [8] Hanny H. Tumbelaka, "A load current sensorless shunt active power filter", Jurnal Teknik Elektro, vol. 7, no. 1, March 2007, pp. 1-7.
- [9] K. Aliouane, "A new space vector control of the three phase PWM Rectifier". POWERENG, Sétubal Portugal, pp. 60-65, 12-14 April 2007.

- [10] J. Y. Hung, W. Gao, and J. C. Hung, "Variable structure control a survey," IEEE Trans. Ind. Electr., vol. 40, 1993, pp. 2-22.
- [11] H. S. Choi, Y. H. Park, Y. S. Cho, and M. Lee, "Global sliding-mode control improved design for a brushless DC motor," IEEE Control Systems Magazine, vol. 21, 2001, pp. 27-35.
- [12] Marcelo C.Cavalcanti, and Gustavo M.S.Azevedo: "Unified Power Conditioner in a Grid Connected Photovoltaic System" Electrical Power Quality and Utilisation, Journal Vol XII, No.2,2006.
- [13] Mariusz Cichowlas, Mariusz Malinowski, Josep Pou, "Active filtering function of three-phase PWM boost rectifier under different line voltage conditions", IEEE transactions on industrial electronics, vol. 52, no. 2, april 2005.
- [14] KNAPCZYK M., PIENKOWSKI K., Sensorless control of AC/DC/AC converter-fed induction motor with sliding-mode observers, Proc. of SME 08, 2008.